frontiers in Marine Science

ORIGINAL RESEARCH
published: 04 April 2019
doi: 10.3389/fmars.2019.00147

Toxicogenomics of Gold Nanoparticles in a Marine Fish: Linkage to Classical Biomarkers

Mariana Teles[1], Felipe E. Reyes-López[2], Joan C. Balasch[2], Asta Tvarijonaviciute[3], Laura Guimarães[1]*, Miguel Oliveira[4]* and Lluis Tort[2]*

[1] CIIMAR-Interdisciplinary Centre of Marine and Environmental Research, Terminal de Cruzeiros do Porto de Leixões, Avenida General Norton de Matos, Matosinhos, Portugal, [2] Department of Cell Biology, Physiology and Immunology, Universitat Autònoma de Barcelona, Barcelona, Spain, [3] Interdisciplinary Laboratory of Clinical Analysis INTERLAB-UMU, Regional Campus of International Excellence Mare Nostrum, University of Murcia, Espinardo, Murcia, Spain, [4] Department of Biology and CESAM, University of Aveiro, Aveiro, Portugal

In the present study, the underlying short-term effects of gold nanoparticles (AuNP, spheres, citrate coated, ∼40 nm) on the hepatic function of gilthead sea bream (*Sparus aurata*) was assessed, using a species-specific enriched oligonucleotide microarray platform (SAQ). Two distinct concentrations of AuNP (0.5 and 50 μg/L) were tested during 24 h waterborne exposure. The transcriptional profile was complemented with outcomes at higher levels of biological organization, including hepatic health indicators and DNA damage indicators. DNA damaging potential of AuNP was assessed in whole peripheral blood, assessing DNA strand breaks (using the comet assay) and chromosome damage (scoring the erythrocytic nuclear abnormalities, ENA). The overall genetic response showed a differential hepatic transcriptional profile, both in terms of number and intensity, of differentially expressed genes (DEG). Concerning the functional pathways that were affected, the main changes found were for gene encoding proteins involved in the response to xenobiotics, oxidoreductase activity, immunomodulation, DNA repair and programmed cell death types I and II. The hepatic health indicators measured revealed that AuNP can induce liver injury, as demonstrated by the plasma alanine aminotransferase (ALT) and aspartate aminotransferase (AST) significantly increased activities after exposure to the highest AuNP concentration (50 μg/L). Exposure to AuNP also caused DNA strand breaks, however, without causing clastogenesis or aneugenesis, since no ENA were detected. Overall, data showed that a short-term exposure to AuNP can modulate gene expression in liver and affects several biochemical/genetic functions in fish.

Keywords: nanotoxicology, microarrays, genotoxicity, *Sparus aurata*, environmental monitoring

OPEN ACCESS

Edited by:
Rathinam Arthur James, Bharathidasan University, India

Reviewed by:
Krishnan Muthukumar, National Institute of Technology, India
Sami Souissi, Lille University of Science and Technology, France

****Correspondence:***
Mariana Teles
mteles0@gmail.com
Laura Guimarães
lguimaraes@ciimar.up.pt
Miguel Oliveira
migueloliveira@ua.pt

Specialty section:
This article was submitted to Marine Pollution, a section of the journal Frontiers in Marine Science

Received: *26 October 2018*
Accepted: *07 March 2019*
Published: *04 April 2019*

Citation:
Teles M, Reyes-López FE, Balasch JC, Tvarijonaviciute A Guimarães L, Oliveira M and Tort L (2019) Toxicogenomics of Gold Nanoparticles in a Marine Fish: Linkage to Classical Biomarkers. Front. Mar. Sci. 6:147. doi: 10.3389/fmars.2019.00147

INTRODUCTION

Human activity along coastal areas is increasing, and waste from industrial processes, household activities, and natural or man-made hazardous substances ultimately reach the marine environment. Moreover, new substances, such as engineered nanoparticles (ENP), are expected to increase in the marine environment in the near future, due to their recent spike of production and use. Gold nanoparticles (AuNP), in particular, are among the most used ENP in

several areas of human activity, such as medicine and water remediation (Cai et al., 2008; Ojea-Jimenez et al., 2012), but little is known in terms of their potential effects to marine organisms. Therefore, it is important to increase the knowledge on their potential toxicity and mechanisms of action, in particular in species of high commercial value used for human consumption.

In the ecotoxicological field, gene expression analysis using DNA microarray technologies can be used as a high-throughput screening tool which offers information on the mechanisms of action of xenobiotics, through the identification of gene expression pathways. Transcriptome profiling allows the assessment of exposure to given contaminants and the subsequent effects, the discovery of new biomarkers of exposure, and the identification of genomic signatures of xenobiotics in aquatic organisms. Meland et al. (2011) used a DNA microarray to examine the effects of short-term exposure to traffic related contaminants in *Salmo trutta* liver, finding several molecular changes that persisted hours after the exposure. In another study, Brinkmann et al. (2016) evaluated the hepatic transcriptional responses in *Rutilus rutilus* following exposure to dioxin-like-compounds, reporting an alteration in genes related with energy metabolism, oogenesis, immune system, apoptosis and response to oxidative stress. So far, few studies have addressed the effects of AuNP in marine organisms, and most of them have been carried out in invertebrates (Joubert et al., 2013; Canesi and Corsi, 2016), with little research performed in marine fish (Teles et al., 2016, 2017). Transcriptomic studies using a fish species as a model are scarce in the nanotoxicology area, even though the molecular effects of zinc oxide or silver nanoparticles have recently been reported in freshwater species, such as *Danio rerio* or *Pimephales promelas* (Garcia-Reyero et al., 2015; Choi et al., 2016). To the authors' knowledge, a single study has, so far, evaluated the effects of AuNP in fish (*D. rerio*) using microarrays (Truong et al., 2013). Recently, an Agilent enriched oligonucleotide microarray platform specific for *Sparus aurata* (SAQ), was developed and validated by the research group (Teles et al., 2013; Boltana et al., 2017). This species has a high economic importance and is cultured in several countries, particularly throughout the Mediterranean area.

A previous study with *S. aurata* showed that citrate coated AuNP affect antioxidant and immune-related homeostasis after 96 h exposure (Teles et al., 2016). The present research work reports the effects of two concentrations of citrate coated AuNP on *S. aurata*'s hepatic transcriptional profile using the SAQ platform. The liver was selected for analysis due to its role in the metabolism and detoxification of xenobiotics and, thus, the target of potential pernicious effects, altering its functions. It has previously been reported that AuNP can have a long blood circulation time and can accumulate in the mammalian liver (Cho et al., 2009). Changes occurring at the molecular level should be anchored to conventional endpoints of toxicity, occurring at levels of biological organization relevant to risk assessment. For this reason, targeted endpoints, namely hepatic health indicators (plasma) and markers of genotoxicity (blood) were also assessed in order to complement the transcriptional data.

MATERIALS AND METHODS

Gold Nanoparticles

In this study, the tested AuNP presented a citrate coating, selected based on the research groups' previous studies with this species (Teles et al., 2016), their application in several areas of activity and previous knowledge of the behavior of these nanoparticles in high ionic strength media (Barreto et al., 2015). AuNP synthesis and characterization followed the protocols described in Barreto et al., 2015. The characteristics of AuNP were as follows: 37 nm diameter; 0.3 polydispersity index and −44.5 zeta potential, which were determined by UV–vis spectrophotometry (Cintra 303, GBC Scientific), dynamic light scattering (Zetasizer Nano ZS, Malvern) and transmission electron microscopy (Hitachi, H9000 NAR). The final concentration of AuNP in the suspension was determined based on their absorption spectra and sizes (Liu et al., 2007; Paramelle et al., 2014) and surface plasmon resonance was analyzed at 0 and 24 h, according to the protocol described in Barreto et al. (2015). Dynamic light scattering data revealed the formation of AuNP- citrate agglomerates/aggregates with sizes up to 600 nm in the first 24 h in saltwater and no variation in the size of AuNP-PVP during 96 h.

Test Organisms and Experimental Setup

S. aurata specimens were obtained from an aquatic culture facility (Cádiz, Spain). The total body weight of fish ranged from 41.3 to 77.4 g, with mean values of 57.1 ± 1.5 g (mean ± SE), and total body length ranged from 14.5 to 18.0 cm, with mean values of 16.4 ± 0.2 cm (mean ± SE). Once in the laboratory, fish were kept in recirculating aerated 250 L aquaria containing artificial saltwater (salinity 31, Ocean Fish, Prodac) at standard laboratory conditions of 20°C on natural photoperiod during a 10 day acclimatization period. Fish were fed daily with a commercial diet (Sorgal, Portugal) at 1% body weight during the acclimatization period. Fish were starved for 24 h prior to the beginning of the experiment and during the experimental assay, in order to avoid the accumulation of organic matter content in the aquaria and the potential interaction of food with AuNP. The experimental setup generally followed the OECD guideline 203 for fish acute toxicity tests and complied with the Directive 2010/63/EU on the protection of animals used for experimental and other scientific purposes. Procedures adopted in the experimental bioassay were previously authorized (N421/2013) by the Portuguese legal authority, "Direção Geral de Veterinária."

The test solutions of AuNP (0.5 and 50 μg/L) were prepared in artificial saltwater and the concentrations were selected based on estimates for environmental levels of AuNP derived for risk assessment, using environmental exposure models and global information on consumer products in the United Kingdom, assuming 10% market penetration (Boxall et al., 2007). Moreover, other authors make reference of levels ranging from 1 to 20 μg/L as environmentally relevant (Baalousha et al., 2016). After acclimatization, the animals were randomly distributed into 80 L duplicated tanks (10 fish per tank at 1 g of fish/L of test solution) and exposed to 0 (control group), 0.5 or 50 μg/L AuNP for 24 h. During the exposure period fish were submitted to similar

laboratory conditions to those used during the acclimation period. After the 24 h of exposure, fish were anesthetized with tricaine methanesulfonate (MS222, Sigma-Aldrich), weighed, and blood was immediately collected from the caudal vasculature using heparinized syringes. Blood smears were directly prepared, and the remaining blood was divided in two aliquots, one used for the Comet assay and the other centrifuged for plasma isolation. Fish livers were then removed, snap frozen in liquid nitrogen and stored at −80°C until analysis. Finally, fish were measured (total length). Biometrical measurements were used to calculate the Fulton's condition factor (K) according to the formula: $K = 100 \times$ body weight (g)/length^3 (cm). Hepatosomatic index (HSI) was presented as a percentage and calculated according to the formula: liver weight (g)/body weight (g) × 100.

Transcriptional Analysis

Total RNA was extracted individually from fish livers using 1 mL of Tri Reagent® (Sigma-Aldrich) per sample, according to the instructions given in the protocol. The concentration of RNA was quantified using a NanoDrop ND-2000 (Thermo Scientific) and RNA integrity and quality checked with the Experion (Automated Electrophoresis Station, Bio-Rad) using the Experion Standard Sens RNA chip (Bio-Rad). Only the samples with an RNA integrity number (RIN) > 7 were used. Transcriptional analysis was carried out using the AquaGenomic *Sparus aurata* oligo-nucleotide microarray (SAQ) platform. The complete information on this platform and experimental design is available through the public repository Gene Expression Omnibus (GEO) (accession numbers GPL13442 and GSE93930, respectively) at the United States National Center for Biotechnology Information (NCBI). A transcriptomic analysis was conducted to determine differences at the expression level between the treatments. Total RNA samples were grouped for the same concentration into three pools of three fish obtaining a total of three pools per condition. One-color microarray was carried out according to the manufacturer's protocols. Briefly, 200 ng of total RNA was reversed transcribed along with spike-in (Agilent One-Color RNA Spike-In kit, Agilent Technologies, United States). The solution was then used as a template for Cyanine-3 (Cy3) labeled cRNA synthesis and amplification with the Quick Amp Labeling kit. Samples of cRNA were purified using the RNeasy micro kit (Qiagen). Dye incorporation and cRNA yield were checked with the NanoDrop ND-2000 Spectrophotometer. 1.5 mg of Cy3-labeled cRNA with specific activity > 6.0 pmol Cy3/mg cRNA was then fragmented at 60°C for 30 min, and the samples were then mixed with hybridization buffer and hybridized to the array (ID 025603, Agilent Technologies, United States) at 65°C for 17 h, using the Gene expression hybridization kit. Washes were conducted as recommended by the manufacturer, using gene expression wash buffers and a stabilization and drying solution (Agilent Technologies, United States). Microarray slides were scanned with Agilent Technologies Scanner model G2505B. Spot intensities and other quality control features were extracted with Agilent's Feature Extraction software version 10.4.0.0 (Agilent Technologies, United States). Quality reports were checked for each array. The extracted raw data were imported and analyzed with GeneSpring (version 14.5 GX software, Agilent Technologies, United States). The 75% percentile normalization was used to standardize the arrays for comparisons, and data were filtered by expression. The principal component analysis (PCA) was used to describe differences among groups. All samples were also analyzed at the gene-level by a reference microarray design approach, to compare the two different AuNP doses using the non-treated fish as a reference group. Expression values with a p-value < 0.05 were considered statistically significant. Biological interpretation of the microarray data was carried out using the free access databases GeneCards® [1] and UniProt[2].

Biochemical Analysis

The hepatic health indicators alanine aminotransferase (ALT), aspartate aminotransferase (AST) and alkaline phosphatase (ALP) were measured in the plasma using commercial kits (Olympus Systems Reagents; Olympus life and Material Science Europe GmbH, Hamburg, Germany) according to the manufacturer's instructions. The analyses were performed with an automatic analyzer (Olympus Diagnostica, GmbH, Hamburg, Germany).

Comet Assay

The comet assay was conducted according to method of Singh et al. (1988) as adapted by Barreto et al. (2017). Diluted blood samples were added to 140 μL of 1% (w/v) low melting point agarose at 40°C, and the mixtures added to the microscope slides were pre-coated with 1% (w/v) of normal melting point agarose. A coverslip was added to each slide, which was then placed on ice for agarose solidification. After solidification, coverslips were removed and the slides immersed (4°C, 1 h) in a lysis solution (2.5 M NaCl, 100 mM EDTA and 10 mM Tris, pH 10.0), containing 1% Triton X-100. Slides were then incubated in alkaline buffer (300 mM NaOH and 1 mM EDTA, pH > 13) for 10 min for DNA denaturation and unwinding. Electrophoresis was performed using the same buffer at 300 mA, 20 V for 30 min. Slides were neutralized in 400 mM Tris buffer pH 7.5, dehydrated with absolute ethanol during 10 s and left to dry for 1 day in the dark. Slides were stained with ethidium bromide (20 μg/mL), covered with a coverslip and analyzed using the Olympus BX41TF fluorescence microscope at 400 × magnification. Slides were randomly analyzed by counting one hundred cells from each slide. Cells were scored visually, according to tail length, into five classes: class 0 - undamaged, without a tail; class 1 - with a tail shorter than the diameter of the head (nucleus); class 2 - with a tail length 1–2 times the diameter of the head; class 3 - with a tail longer than twice the diameter of the head; class 4 - comets with no heads. A damage index (DI) expressed in arbitrary units was assigned to each replicate (for 100 cells) and consequently for each treatment, according to the damage classes, using the formula:

$$DI = (0 \times n0) + (1 \times n1) + (2 \times n2) + (3 \times n3) + (4 \times n4)$$

[1] www.genecards.org

[2] www.uniprot.org

where n = number of cells in each class analyzed. The DI of each treatment could range from 0 (completely undamaged: 100 cells × 0) to 400 (maximum damage: 100 cells × 4) (Andrade et al., 2004). A percentage of DNA damage relative to the control was calculated.

Erythrocytic Nuclear Abnormalities Assay

Blood smears were fixed in 100% methanol for 10 min and stained with 5% Giemsa for 30 min, and the erythrocytic nuclear abnormalities (ENA) assay was carried out in mature erythrocytes according to the method adapted by Pacheco and Santos (1996). The following nuclear lesion categories were considered: micronuclei (M), lobed nuclei (L), dumbbell shaped or segmented nuclei (S), and kidney shaped nuclei (K). The final result was expressed as the mean value (‰) of the sum of all individual lesions observed.

Data Analysis

For the microarray data, a statistical analysis (unpaired t-test) was done using the GeneSpring software GX 14.5 to detect differentially expressed genes (DEG, $p < 0.05$) between control group and groups exposed to different concentrations of AuNP. For all the other parameters, statistical analysis was performed using the IBM SPSS Statistics 19 software. Differences between groups were tested using a one-way ANOVA followed by the Tukey's test ($p < 0.05$).

RESULTS

No mortality was recorded during the experimental assay. Fulton's condition factor (K) and hepatosomatic index (HSI) were not significantly different between experimental groups (data not shown).

Transcriptional Regulation in the Liver

The PCA divided the data set into three principal components revealing a clear differential gene expression pattern among treatments (**Figure 1A**). This allowed grouping all samples into three well defined clusters corresponding to the control, 0.5 and 50 μg/L groups. The transcriptome profiles of individuals treated with 0.5 and 50 μg/L of AuNP were significantly different both in transcript number and intensity of the response. Overall, 939 genes were found differentially expressed ($p < 0.05$) (Supplementary Material). Concerning the exclusive DEG for each concentration compared to the control group (**Figure 1B**), 365 transcripts were modulated in fish exposed to the lowest concentration (0.5 μg/L), 574 transcripts were exclusive of the highest concentration (50 μg/L), and 47 transcripts were common to both treatments. From the 365 DEG exclusive of the lowest concentration, 236 were upregulated and 129 downregulated; whereas for the highest concentration 279 DEG were upregulated and 295 DEG were downregulated. From 47 common DEG, 18 transcripts were upregulated, and 29 transcripts were downregulated for 0.5 μg/L; whereas 20 were upregulated and 27 downregulated for 50 μg/L. A stringency

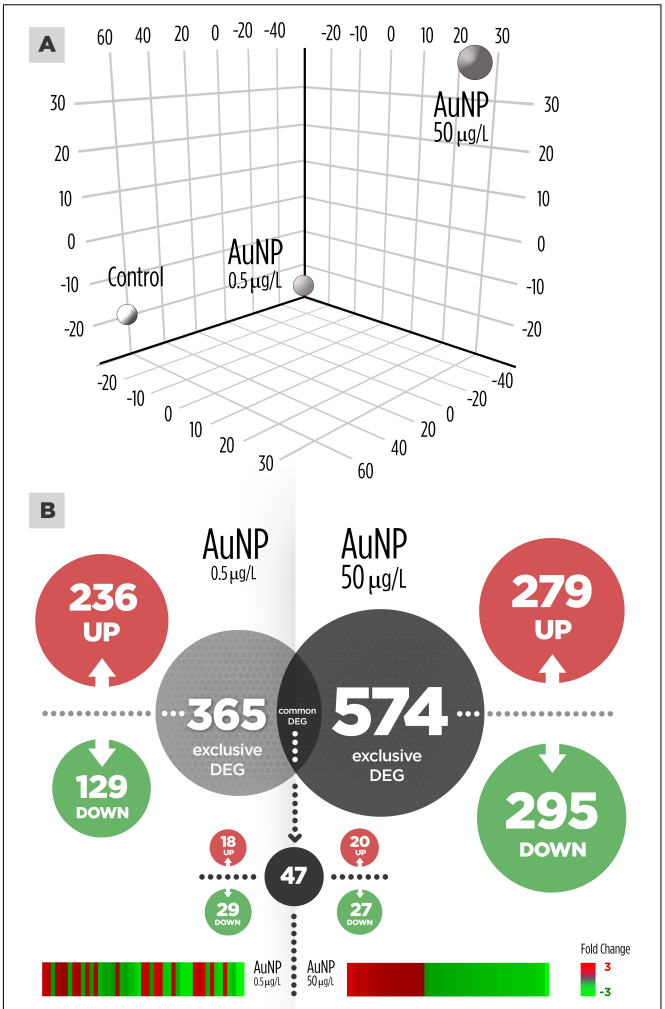

FIGURE 1 | Transcriptional overview in the liver of *Sparus aurata* after 24 h exposure to gold nanoparticles (AuNP). **(A)** Principal Component Analysis (PCA) 3D plot of the liver samples grouped by treatment. **(B)** Venn diagram representing differentially expressed genes (DEG). Light gray circle: 365 DEG after exposure to 0.5 μg/L AuNP. Dark gray circle: 574 DEG after exposure to 50 μg/L AuNP.

cut-off was adopted and selected genes that had a $p < 0.05$ and absolute fold change (AFC) > 1.5 are presented in **Tables 1**, **2**. Transcriptomic and gene ontology analysis revealed that 24 h exposure to 0.5 μg/L, induced changes in transcripts mainly related with the sensing and metabolism of xenobiotics, immune response, DNA repair and apoptosis regulation and several factors that regulate transcription, DNA processing and translation processes. Endocrine regulation and carbohydrate metabolism were downregulated by 0.5 μg/L AuNP. The highest AuNP concentration, 50 μg/L, induced an upregulation of transcripts associated with the response to xenobiotics, electron transport chain, immune response and DNA repair. Many genes involved in autophagy and cellular stress, lipid and protein metabolism, as well as several factors that regulate transcription, DNA processing and translation regulation were also upregulated

TABLE 1 | Differentially expressed genes for 0.5 μg/L AuNP.

Functional pathway	Upregulated genes	FC	*p* value	Function
Response to xenobiotics/ Oxidoreductase activity	Selenium binding protein 1	1,45	0,023	Sensing of reactive xenobiotics in the cytoplasm
	L-2-Hydroxyglutarate dehydrogenase (L2HGDH)	2,89	0,017	Oxidoreductase activity
	Sulfotransferase 1 isoform 3 (SULT1A3)	1,75	0,033	Phase II biotransformation
	Cytochrome P450 2N (CYP2N)	1,67	0,012	Oxidoreductase activity (xenobiotic)
	Cytochrome P450 2P11 (CYP2P11)	1,31	0,019	Oxidoreductase activity (xenobiotic)
Immune response	CC Chemokine	2,46	0,045	Innate immunity
	Novel NACHT domain containing protein (NLRP3)	2,19	0,028	PAMPS and DAMPS sensing
	Tyrosine-protein kinase ZAP70 (ZAP-70)	2,00	0,016	Adaptive immunity
	Alpha-2, 6-sialyltransferase (ST6GAL1)	1,81	0,037	Immune response
	MHC class I antigen (HLA-A)	1,51	0,011	Antigen presentation
	Integrin beta 1 binding protein 3	1,47	0,014	Immune response
	Myeloid differentiation factor 88 (MYD88)	1,33	0,030	Pathogen recognition
DNA repair/Apoptosis regulation	WD repeat-containing protein 60 (WDR60)	2,07	0,027	Apoptosis
	Perforin 1	2,06	0,025	Apoptosis
	Fanconi anemia group F protein (FANCF)	1,84	0,018	DNA repair
	Mismatch repair protein Msh6 (MSH6)	1,78	0,031	DNA repair, Apoptosis
	Chromosome condensation 1	1,67	0,031	DNA repair
Transcription, DNA processing and translational regulation	Serine/arginine-rich splicing factor 12 (SRSF12)	2,18	0,002	Splicing factor
	Myocyte enhancer factor 2A (MEF2A)	2,03	0,005	Transcription factor
	Emx2 homeoprotein (EMX2)	1,78	0,026	Regulation of transcription
	Eukaryotic translation initiation factor 4E (EIF4E)	1,71	0,033	Proto-oncogene
	Transcription Factor E2F8 (E2F8)	1,69	0,021	Transcription factor, cell proliferation
	Ribosomal protein L13a (RPL13a)	1,67	0,039	Translation regulation
Other	Erythrocyte membrane protein band 3-like 1 (SLC4A1)	2,35	0,046	Cellular ion homeostasis
	Ethanolamine kinase 1 (ETNK1)	1,71	0,028	Lipid metabolism
	Mitotin	1,63	0,016	DNA replication initiation
	Plakophilin 3 (PKP3)	1,55	0,039	Cell adhesion
	ADP ribosylation factor-like protein 2 (ARL2)	1,52	0,017	Cell cycle
	Intraflagellar transport 81 (IFT81)	1,51	0,045	Cytoskeleton rearrangement
	Talin 1 (TLN1)	1,50	0,048	Cytoskeleton organization
Functional pathway	Downregulated genes	FC	*p* value	Function
Carbohydrate metabolism	Monoacylglycerol O-acyltransferase 2 (MOGAT2)	−1,64	0,021	Carbohydrate and lipid metabolism
	Glucose dehydrogenase	−1,34	0,036	Carbohydrate metabolism
Other	Sec61 beta subunit (SEC61B)	−1,94	0,010	Cell growth
	Torsin 1A interacting protein 2 (TOR1AIP2)	−1,88	0,045	Endoplasmic reticulum organization
	Protein kinase raf 1 (RAF1)	−1,84	0,036	MAPK cascade
	C-ski protein (class I) (c-ski)	−1,62	0,024	Proto-oncogene. Repressor of TGFb
	Vacuolar protein sorting-associating protein 4B (VPS4B)	−1,61	0,016	Cell cycle
	Erythrocyte protein band 4.1-like 3 (EPB41L1)	−1,59	0,017	Cell growth
	Thyroid transcription factor 1-associated protein 26 homolog (ccdc59)	−1,59	0,023	Transcription factor

in the liver of fish exposed to 50 μg/L AuNP. Concerning the downregulated transcripts, the main classes affected were endocrine regulation, immune response and cell death.

Hepatic Health Indicators and Genotoxicity

The analysis of the three hepatic health indicators measured in the plasma of fish exposed to AuNP for 24 h, revealed that ALP was at control levels but AST and ALT levels were significantly higher in fish exposed to 50 μg/L, when compared to the control and to 0.5 μg/L AuNP treated groups. Both AuNP concentrations induced significant DNA damage when compared to the control, with the highest concentration tested inducing higher DNA damage than the lowest (**Figure 2**). The damage classes were analyzed individually, considering the GDI parameter (**Table 3**). In fish exposed to 0.5 μg/L AuNP, damaged nucleoid of classes 1

TABLE 2 | Differentially expressed genes for 50 μg/L AuNP.

Functional pathway	Upregulated genes	FC	*p* value	Function
Response to xenobiotics/ Oxidoreductase activity	ATP-binding cassette subfamily F member 2 (ABCF2)	2.36	0.001	Enhances excretion of xenobiotics
	Aryl hydrocarbon receptor 2 (AhR2)	1.38	0.049	Xenobiotic receptor
	Cytochrome b-c1 complex subunit 6 (UQCRH)	1.54	0.027	Electron transport chain
	Cytochrome b-c1 complex subunit Rieske (UQCRFS1)	1.51	0.031	Electron transport chain
	Cytochrome c oxidase subunit Vaa	1.51	0.029	Electron transport chain
	NADH dehydrogenase iron-sulfur protein 3, mitochondrial (NDUS3)	1.30	0.026	Electron transport chain
Immune response	FBP32	4.02	0.050	Pathogen recognitions (F-type lectin)
	Coiled coil domain containing 86 (CCDC86)	1.84	0.026	Immune response. Cytokine-induced protein
Response to stress/Autophagy	Chromatin modifying protein 4C (CHMP4C)	1.94	0.031	Autophagy
	HSPC171 protein	1.79	0.008	Autophagy and endoplasmic reticulum stress
	HSC70	1.55	0.040	Response to stress. Chaperone mediated Autophagy
	Stromal cell-derived factor 2-like protein 1 (SDF2L1)	1.86	0.023	Endoplasmic reticulum inducible stress
	Chromatin modifying protein 4B (CHMP4B)	1.42	0.038	Autophagia, protein transport
Lipid/protein metabolism	Farnesyl pyrophosphate synthetase	3.05	0.007	Lipid metabolism
	Isopentenyl-diphosphate delta-isomerase 1 (IDI1)	2.73	0.042	Lipid metabolism
	Microsomal triglyceride transfer protein (MTTP)	1.53	0.003	Lipid metabolism
	Pitrilysin metalloproteinase 1 (PITRM1)	1.96	0.032	Protein catabolism
	Threonyl tRNA synthetase (TARS)	1.89	0.011	Protein biosynthesis
	Transmembrane protein 147 (TMEM147)	1.87	0.042	Protein destabilization
	Dipeptidyl peptidase 3 (DPP3)	1.82	0.018	Protein catabolism
	26S protease regulatory subunit 6A (PSMC3)	1.55	0.022	Protein regulation
Transcription, DNA processing and translational regulation	Early growth response 1 (EGR1)	4.05	0.045	Regulates the response to DNA damage
	Exosome complex exonuclease RRP45	1.97	0.036	RNA processing
	WD repeat-containing protein 75 (WDR75)	1.90	0.039	rRNA processing
	Small nuclear ribonucleoprotein Sm D2 (SNRPD2)	1.78	0.003	mRNA processing
	Transducin beta like 3 (TBL3)	1.73	0.042	rRNA processing
	Eukaryotic translation initiation factor 4 gamma 2 (EIF4G1)	1.59	0.030	Translation regulation
	WW domain binding protein 11 (WBP11)	1.54	0.038	RNA processing
	Lupus La protein homolog B (ssb-b)	1.54	0.021	RNA processing
	Helicase MOV10	1.50	0.045	Regulation of transcription
	DNA damage inducible transcript 4 protein (DDIT4)	2.31	0.014	Response to DNA damage
Other	Bystin (BYSL)	2.23	0.029	Cell cycle regulation
	WD repeat domain 3 (WDR3)	2.04	0.016	Cell cycle regulation
	UMP-CMP kinase (CMPK1)	2.00	0.038	Nucleic acid biosynthesis
	Luteinizing hormone receptor (LHCGR)	1.92	0.032	Hormone mediated signaling pathway
	Glutathione reductase, mitochondrial precursor	1.20	0.028	Oxidative stress
Functional pathway	Downregulated genes	FC	*p* value	Function
Immune response	Chemokine CK-1	−3.69	0.011	Immune response
	C-type lectin domain family 4 member E (CLEC4E)	−1.95	0.006	Immune system response. Pathogen recognition
	WD repeat and FYVE domain-containing protein 1 (Wdfy1)	−1.72	0.037	Positively regulates TLR3- and TLR4
	Complement component C4 (C4)	−1.55	0.019	Complement pathway
Cell death (apoptosis)	Adapter Protein GRB2 (GRB2)	−2.69	0.000	May trigger active programmed cell death
	Tumor necrosis factor receptor superfamily member 16 (NGFR)	−1.63	0.025	Apoptosis
	Programmed cell death 7	−1.55	0.015	Apoptosis
	Mitogen-activated protein kinase 7 (MAP2K7)	−1.50	0.049	Apoptosis

(Continued)

TABLE 2 | Continued

Functional pathway	Upregulated genes	FC	*p* value	Function
Other	Elastase-like serine protease	−2.23	0.036	Protease
	HRAS-like suppressor, isoform CRA_b	−2.21	0.003	Tumor suppressor
	Adenylate cyclase type 6 (ADCY6)	−2.00	0.027	Energy metabolism
	Geminin (GMNN)	−1.92	0.025	Cell cycle regulation
	Alpha-actinin 1 (ACTN1)	−1.92	0.022	Cytoskeleton protein
	3-Oxoacid CoA transferase 1a (OXCT1)	−1.88	0.041	Enzyme (transferase)
	Septin 9 (SEPT9)	−1.87	0.024	Cell cycle regulation
	Deoxyribonuclease gamma precursor	−1.78	0.009	DNA catabolic process
	Bloodthirsty	−1.71	0.028	Erythrocyte differentiation
	Arginine/serine-rich coiled-coil protein 2 (RSRC2)	−1.67	0.032	Poly(A) RNA binding
	CEF10	−1.63	0.046	Cell growth regulation
	Ankyrin repeat-containing protein	−1.57	0.045	Transcription factor

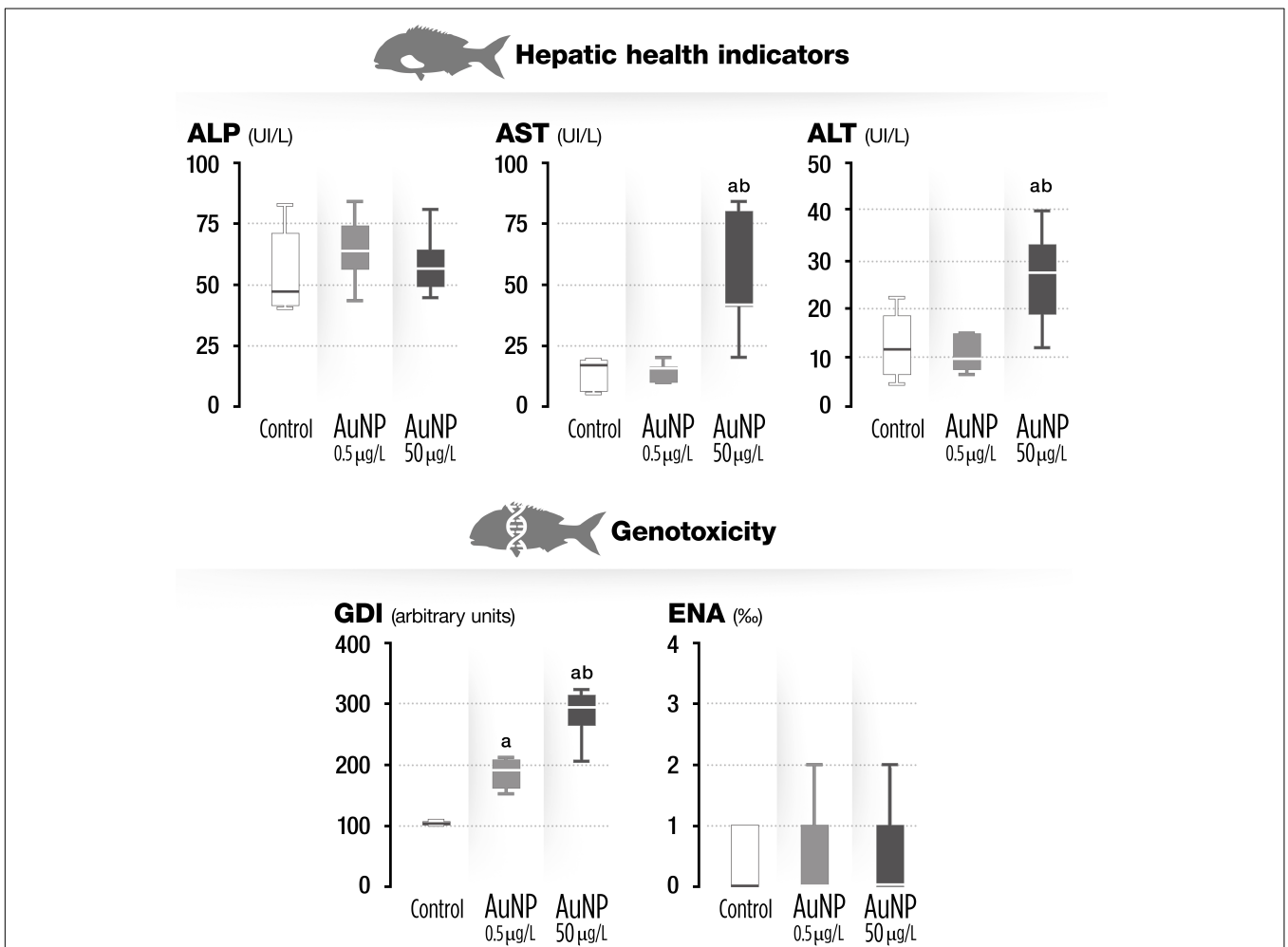

FIGURE 2 | Plasma alkaline phosphatase (ALP), plasma aspartate aminotransferase (AST), plasma alanine transaminase (ALT), blood genetic damage indicator (GDI) and erythrocytic nuclear abnormalities (ENA) frequency of *Sparus aurata* exposed to gold nanoparticles (AuNP) for 24 h. Values represent the mean ± standard error. Significant differences ($p < 0.05$) are: a *versus* control; b *versus* 0.5 µg/L AuNP.

and 2 were significantly higher than in the control group, whereas in fish exposed to 50 µg/L AuNP, significant increases in the classes 1, 2, 3, and 4 were found when compared to the control and 1, 3, and 4 when compared to the 0.5 µg/L treated groups. Considering ENA assay (**Figure 2**), no significant differences were observed between the groups.

TABLE 3 | Mean frequencies (%) of damaged nucleoid classes' ± standard error (SE).

Condition	0	1	2	3	4
Control	0.3 ± 1.1	96.1 ± 1.1	2.9 ± 0.9	0.8 ± 0.6	0.0 ± 0.0
0.5 μg/L	0.0 ± 0.0	32.4 ± 5.7[a]	49.4 ± 5.2[a]	17.3 ± 4.4	0.6 ± 0.4
50 μg/L	0.0 ± 0.0	0.8 ± 0.5[ab]	28.8 ± 9.8[a]	57.3 ± 8.7[ab]	13.6 ± 4.2[ab]

Numbers 0–4 correspond to DNA damage classes (GDI). Groups with different superscripts differ significantly at $p < 0.05$. a, versus control; b: 0.5 versus 50 μg/L.

DISCUSSION

This study that aimed to study the potential consequences of AuNP (citrate-capped spheres, ∼40 nm) exposure on the hepatic transcriptome of gilthead sea bream, revealed that 0.5 and 50 μg/L AuNP trigger different gene expression profiles, both in the number of up- or downregulated transcripts as in the associated functional pathways. The magnitude of changes was lower in animals exposed to the lowest AuNP concentration, as demonstrated by the lower number of DEG (up- or downregulated) found in this concentration. In fact, the number of downregulated transcripts for the highest AuNP concentration was double those found in the lowest tested concentration. This effect can be related to the fact that, in general, at low doses there is an activation of pathways that compensates the stress induced by the toxicant exposure, protecting the organism from its potential toxicity and ensuring survival. Higher concentrations or longer exposures to stress inducing agents may lead to a refractory or tolerant state, often accompanied by a downregulation of genes and/or pathways. Moreover, organisms start to become unable to adapt or compensate, leading to the start of a general toxicity situation.

Xenobiotic Metabolism

Overall, the present study's results demonstrate that low doses of AuNP, despite being considered as non-toxic, affects the short-term transcriptomic profile of the hepatic function of *S. aurata*. Upregulation of genes involved in the sensing and metabolism of xenobiotics, such as cytochrome P450 2N (CYP2N) and CYP2P11 (for 0.5 μg/L AuNP) was found. These genes belong to the cytochrome P450 subfamily which consists of a large number of enzymes involved in the detoxification of endogenous and exogenous compounds, both in mammals and fish. In the same experimental group, the expression of sulfotransferase 1 isoform 3, SULT1A3 (a phase II biotransformation enzyme that catalyzes the conjugation of many hormones, neurotransmitters and xenobiotics) was also upregulated (Gamage et al., 2006). In fish exposed to the highest concentration of AuNP, the upregulation of aryl hydrocarbon receptor 2 (AhR2) was also observed. The AhR is a ligand-activated transcription factor that controls the expression of a diverse set of genes (Beischlag et al., 2008). In previous studies, AhR2 gene expression was shown to be increased in the liver of *Acipenser transmontanus* after exposure to dioxin-like compounds (Doering et al., 2014). However, in the embryos of *D. rerio*, AhR2 gene expression decreased after silver nanoparticles (AgNP) (10 nm) exposure (from four to 96 hpf) (Xin et al., 2015). Also, the ATP-binding cassette subfamily F member 2 (ABCF2) gene was upregulated in the liver of fish exposed to the highest AuNP concentration. This gene encodes a member of the ATP-binding cassette (ABC) transporter superfamily (Chueh et al., 2014), being the main efflux pump also involved in detoxification pathways, including in the detoxification of heavy metals. Similarly, Chueh et al. (2014) found an increased expression of several ABC transporters after MRC5 cell line's (human normal lung fibroblasts) 24 h treatment with AuNP (360 ng/mL). Altogether, the data from the present study indicate that AuNP modulates metabolic genes/pathways in the liver, which probably account for their metabolism and detoxification/excretion. This is in accordance with previous results found in rats treated with a single intravenous injection of 15 μg/mL AuNP-citrate (20 nm) (Balasubramanian et al., 2010) and in *D. rerio* fed daily with 36–106 ng Au/fish/day (50 nm) (Geffroy et al., 2012), where the authors found an increased expression of genes involved in detoxification processes. Moreover, several genes belonging to the electron transport chain, such as cytochrome b-c1 complex subunit 6 and cytochrome b-c1 complex subunit Rieske were upregulated for the highest concentration tested, which indicates an activation of the mitochondrial electron transport chain and the potential overproduction of reactive oxygen species (ROS).

Immune Response

In the present study, both TLR-related pro-inflammatory myeloid differentiation factor 88 (MyD88) and novel NACHT domain containing protein (NLRP3) were upregulated in the liver of *S. aurata* exposed to 0.5 μg/L AuNP. Toll like receptors (TLR) are pattern-recognition receptors (PRRs) associated to the early immune response that, by sensing microbial specific structures and danger-associated molecular patterns (PAMPs and DAMPs, respectively) trigger cell signaling cascade activators such as MyD88. The NLRP3 protein constitutes the major sensor protein of the inflammasome, a multiprotein cytosolic complex required for the onset of cytokine-related inflammatory responses (Lamkanfi and Dixit, 2011). Notwithstanding the absence of direct orthologs of NLRP3 in fish, it has been suggested that *S. aurata* possesses an NLRP3-like inflammasome complex that enables the development of pro-inflammatory reactivity (Compan et al., 2012). Therefore, the obtained results suggest that AuNP may activate both the TLR and inflammasome signaling cascade in *S. aurata*. The exposure to 0.5 μg/L induced an upregulation of ZAP70, the antigen-presenting major histocompatibility complex class I molecule (MHC-I) and CC- chemokines. The cross-linking between MHC class I molecules and T cells promotes the activation of a signal-transduction cascade, leading to the activation of tyrosine kinases. In mammals, MHC class I is able to activate ZAP70 in T cells after MHC class I ligation (Skov et al., 1997), and CC-chemokines promote cell recruitment to the site of infection, tissue maintenance, or development-associated processes. This opens up the possibility that the waterborne exposure of *S. aurata* to 0.5 μg/L AuNP triggered an MHC-I-mediated activation of T cell signaling cascades and promoted cell recruitment. For 50 μg/L AuNP, a shift toward a

downregulation of immune genes, when compared to 0.5 μg/L, was found. The only upregulated gene classified with an immune function was FBP32, an F-type lectin abundantly expressed in the liver of *Morone saxatilis* after an immune challenge (Odom and Vasta, 2006). Both complement components C4 and chemokine CK1 were downregulated, and thus impaired the inflammatory progression and the cellular crosstalk needed for antigen recognition processes. Globally, the data from this study show that exposure to AuNP modulates the expression of several immune-related genes and this differential effect seems to be AuNP dose-dependent. While the low concentration upregulates, genes related to several immunological processes, the high concentration seems to have immune-suppressive effects. Present results corroborate previous findings showing the misregulation of pathways related to inflammation and immune responses in zebrafish embryos exposed to AuNP (Truong et al., 2013).

Genotoxicity

An upregulation of transcripts involved in DNA repair, such as fanconi anemia group F protein (FANCF) and mismatch repair protein (Msh6) was found, especially for the low concentration. FANCF gene encodes for a DNA repair protein that may operate in a post-replication repair or a cell cycle checkpoint function, and may be implicated in interstrand DNA cross-link repair and maintenance of normal chromosome stability (O'Rourke and Deans, 2016). On the other hand, msh6 gene encodes for a protein involved in DNA mismatch repair (MMR) (Edelbrock et al., 2013). The present study results corroborate previous findings showing an upregulation of genes (*gaad* and *rad 51*) involved in DNA repair function in zebrafish exposed to 0.25 μg/L of 14 nm AuNP-citrate over 20 days (Dedeh et al., 2015). Moreover, the results of a cDNA microarray analysis showed an upregulation of FANCF in MCR-5 cells treated with 360 ng/mL AuNP (Chueh et al., 2014). The activation of genes involved in DNA damage response and repair, indicate that AuNP caused DNA damage, which may activate pathways that minimize this damage to maintain genetic integrity and cell survival (Singh et al., 1988). This hypothesis is supported by the studied genotoxicity biomarkers that showed a dose-dependent increase in blood DNA strand breaks, despite the absence of chromosome clastogenesis. The distinct response observed for the two tested concentrations indicate that while the lowest concentration provokes DNA damage, which activates the DNA repair machinery, this effect is increased at high concentration, probably generating an excessive response and limiting the repair capacity and thus generating more DNA damage. This suggests that, for the low concentration, the activation of DNA repair machinery is limiting the potential genetic damage generated by the exposure to AuNP. By contrast, for the high AuNP concentration, the protective effect of the DNA repair machinery is overwhelmed, and genetic damage is observed as a consequence. Nevertheless, this DNA damage is likely compensated by other alternative repair strategies that can be the responsible for the absence of ENA. Hence, the genotoxicity results obtained for the highest concentration tested, supports previous studies and the idea that DNA chain damage measured by comet assay does not necessarily cause chromosomal clastogenesis/aneugenic events (Costa et al., 2011). These genomic alterations may be caused by direct action of AuNP through their binding to DNA or indirectly, through the generation of oxidative stress that can lead to DNA strand breaks. To date, there are few studies about the interaction of AuNP with the DNA (Geffroy et al., 2012; Dedeh et al., 2015). In zebrafish, it was previously shown that AuNP exposure (through the diet or contaminated sediments) induced genotoxicity measured with a random amplified polymorphic DNA (RAPD)-based methodology (Geffroy et al., 2012; Dedeh et al., 2015). Moreover, it was found that administration of AuNP causes DNA damage in rats measured by the comet assay (Cardoso et al., 2014) and can induce cell death (Borges et al., 2008).

In the present study, a modulation of genes belonging to the programmed cell death type I (apoptosis) and II (autophagy) was shown. Thus, for the lowest AuNP concentration, an upregulation of apoptosis related genes, such as perforin 1, a gene encoding for proteins that promote cytolysis and apoptosis of target cells by facilitating the uptake of cytotoxic granzymes (Krähenbühl and Tschopp, 1991) was found. Whereas for the highest AuNP concentration, an upregulation of genes linked to autophagy and endoplasmic reticulum stress (e.g., HSPC171 protein and HSC70), together with a downregulation of apoptosis related genes (e.g., programmed cell death 7) was observed. Apoptosis and autophagy have previously been shown to occur in response to treatments with nanomaterials (Popp and Segatori, 2015). These processes are of high importance to organisms. Apoptosis is critically important for the survival of multicellular organisms by getting rid of damaged or infected cells that may interfere with normal function (Portt et al., 2011) whereas autophagy is an important multifunctional process, which cells use to recycle cellular constituents, a process that plays an important role in normal cellular homeostasis (Popp and Segatori, 2015). Under the present circumstances, it seems that these processes are activated to compensate the stress caused by the exposure to AuNP, in agreement with previous suggestions that autophagy is activated upon internalization of engineered nanomaterials as a protective response to what is perceived as foreign or toxic (Popp and Segatori, 2015). In the present study, it was shown that exposure to the lowest concentration of AuNP upregulated apoptosis-related genes and the highest AuNP concentration upregulated autophagy and downregulated apoptosis. One way autophagy can serve as an antiapoptotic process is by removing damaged cellular components such as ER that contains an excess of unprocessed proteins due to ER stress (Portt et al., 2011). Thus, autophagy may be capable of protecting from extreme stress, in this case represented by the highest concentration of AuNP tested. These results are in agreement with previous findings, where AuNP exposure induced autophagy in different mammalian cell lines (Chueh et al., 2014). For the highest AuNP concentration, an upregulation of genes related to energy metabolism, such as Pitrilysin metalloproteinase 1 gene, was also found, which suggests an activation of proteolysis, probably supplying amino acids as substrates for gluconeogenesis and allowing the elimination of damaged proteins. For both concentrations upregulation of several genes encoding transcription factors were observed, corroborating that AuNP activate the transcriptional machinery resulting in the modulation of several key pathways

in the liver of *S. aurata*. Moreover, there are several up or downregulated genes that correspond to transcripts with an unknown function (**Supplementary Table S1**). Therefore, further studies are needed to determine the nature of these genes and their role and implications in fish response to nanoparticles exposure.

Other Endpoints

The hepatic health indicators evaluated in the present study revealed an unaltered LSI and ALP, together with an increase in AST and ALT activities in the plasma of *S. aurata*. These enzymes are mainly contained within liver cells and to a lesser degree in the muscle cells. Upon liver damage, hepatic cells spill these enzymes into the blood, raising the AST and ALT enzyme blood levels, signaling liver injury. Accordingly, data suggest that the highest concentration of AuNP generates liver damage and adversely affects liver function. These results are consistent with previous reports that demonstrated increased hepatic enzymes in mice treated with AuNP (Zhang et al., 2011).

CONCLUSION

The present study allowed for a better understanding of the modes of action of AuNP in marine fish. Overall, fish showed sensitivity to short-term waterborne exposure and concentration specific responses. Despite the low concentrations tested, AuNP demonstrated the ability to modulate transcripts associated with sensing and metabolism of xenobiotics, immune function, DNA repair and programmed cell death. The importance of different concentrations in the biological response to nanoparticles is clearly shown in this study, as demonstrated, for example, in terms of immune related transcripts, which upon exposure to the lowest tested concentration suggests immune stimulation, and the highest concentration immune suppression. Although fish present several mechanisms to prevent molecular alterations from leading to pernicious effects at higher levels of biological organization, the present study shows that marine fish may suffer detrimental effects from nanoparticles released into the environment, justifying further studies on the effects of nanoparticles (e.g., metallic and polymeric) on marine fish.

DATA AVAILABILITY

All datasets generated for this study are included in the manuscript and/or the **Supplementary Files.**

AUTHOR CONTRIBUTIONS

MT, MO, LG, and LT designed the experiments. FRL did the microarrays. MT and MO set up and performed the experiments. AT did the biochemical analysis. MT, FRL, and JCB did the microarrays analysis. MO and MT did the comet assay. MT analyzed all the results and wrote the article. JB prepared the figures. All authors have read and approved the manuscript for publication.

FUNDING

This research was supported through the COMPETE (Operational Competitiveness Program) and national Portuguese funds through the Foundation for Science and Technology (FCT), under the project "NANOAu – Effects of Gold Nanoparticles to Aquatic Organisms" (FCTPTDC/MAR-EST/3399/2012) (FCOMP-01-0124-FEDER-029435); CESAM: UID/AMB/50017/2019 and by the "Plan Nacional de Investigación", Government of Spain (AGL2013-48835-C2-2-R). MT has a post-doctoral fellowship from FCT (SFRH/BPD/109219/2015) supported by the European Social Fund and national funds from the "Ministério da Educação e Ciência (POPH – QREN – Tipologia 4.1)" of Portugal. AT was supported by the Program "Ramon y Cajal" of 'Ministerio de Economia y Competitividad', Spain, through a postdoctoral grant. MO has financial support of the program Investigador FCT, co-funded by the Human Potential Operational Programme and European Social Fund (IF/00335/2015).

ACKNOWLEDGMENTS

A. Barreto, C. Fierro-Castro, and I. Jerez-Cepa are thanked and acknowledged for their support during the sampling.

SUPPLEMENTARY MATERIAL

The Supplementary Material for this article can be found online at: https://www.frontiersin.org/articles/10.3389/fmars.2019.00147/full#supplementary-material

TABLE S1 | Complete list of transcripts differentially regulated ($p < 0.05$) in the liver of *Sparus aurata* after 24 h of waterborne exposure to gold nanoparticles (AuNP) when compared to control group.

REFERENCES

Andrade, V. M., Silva, J., Silva, F. R., Heuser, V. D., Dias, J. F., Yoneama, M. L., et al. (2004). Fish as bioindicators to assess the effects of pollution in two southern Brazilian rivers using the Comet assay and micronucleus test. *Environ. Mol. Mutagen.* 44, 459–468. doi: 10.1002/em.20070

Baalousha, M., Sikder, M., Prasad, A., Lead, J., Merrifield, R., and Thomas Chandler, G. (2016). The concentration-dependent behaviour of nanoparticles. *Environ. Chem.* 13, 1–3. doi: 10.1071/EN15142

Balasubramanian, S. K., Jittiwat, J., Manikandan, J., Ong, C. N., Yu, L. E., and Ong, W. Y. (2010). Biodistribution of gold nanoparticles and gene expression changes in the liver and spleen after intravenous administration in rats. *Biomaterials* 31, 2034–2042. doi: 10.1016/j.biomaterials.2009.11.079

Barreto, A., Luis, L. G., Soares, A., Paiga, P., Santos, L., Delerue-Matos, C., et al. (2017). Genotoxicity of gemfibrozil in the gilthead seabream (Sparus aurata). *Mutat. Res.* 821, 36–42. doi: 10.1016/j.mrgentox.2017.05.011

Barreto, Â, Luis, L. G., Girão, A. V., Trindade, T., Soares, A. M. V. M., and Oliveira, M. (2015). Behavior of colloidal gold nanoparticles in different ionic strength media. *J. Nanopart. Res.* 17:493. doi: 10.1007/s11051-015-3302-0

Beischlag, T. V., Luis Morales, J., Hollingshead, B. D., and Perdew, G. H. (2008). The aryl hydrocarbon receptor complex and the control of gene expression. *Crit. Rev. Eukaryot. Gene Expr.* 18, 207–250. doi: 10.1615/CritRevEukarGeneExpr.v18.i3.20

Boltana, S., Castellana, B., Goetz, G., Tort, L., Teles, M., Mulero, V., et al. (2017). Extending immunological profiling in the gilthead sea bream, sparus aurata, by enriched cDNA library analysis, microarray design and initial studies upon the inflammatory response to PAMPs. *Int. J. Mol. Sci.* 18:E317. doi: 10.3390/ijms18020317

Borges, H. L., Linden, R., and Wang, J. Y. J. (2008). DNA damage-induced cell death: lessons from the central nervous system. *Cell Res.* 18, 17–26. doi: 10.1038/cr.2007.110

Boxall, A. B. A., Tiede, K., and Chaudhry, Q. (2007). Engineered nanomaterials in soils and water: how do they behave and could they pose a risk to human health? *Nanomedicine* 2, 919–927. doi: 10.2217/17435889.2.6.919

Brinkmann, M., Koglin, S., Eisner, B., Wiseman, S., Hecker, M., Eichbaum, K., et al. (2016). Characterisation of transcriptional responses to dioxins and dioxin-like contaminants in roach (Rutilus rutilus) using whole transcriptome analysis. *Sci. Total Environ.* 541, 412–423. doi: 10.1016/j.scitotenv.2015.09.087

Cai, W., Gao, T., Hong, H., and Sun, J. (2008). Applications of gold nanoparticles in cancer nanotechnology. *Nanotechnol. Sci. Appl.* 1, 17–32. doi: 10.2147/NSA.S3788

Canesi, L., and Corsi, I. (2016). Effects of nanomaterials on marine invertebrates. *Sci. Total Environ.* 565, 933–940. doi: 10.1016/j.scitotenv.2016.01.085

Cardoso, E., Rezin, G. T., Zanoni, E. T., de Souza Notoya, F., Leffa, D. D., Damiani, A. P., et al. (2014). Acute and chronic administration of gold nanoparticles cause DNA damage in the cerebral cortex of adult rats. *Mut. Res.* 766–767, 25–30. doi: 10.1016/j.mrfmmm.2014.05.009

Cho, W. S., Cho, M., Jeong, J., Choi, M., Cho, H. Y., Han, B. S., et al. (2009). Acute toxicity and pharmacokinetics of 13 nm-sized PEG-coated gold nanoparticles. *Toxicol. Appl. Pharmacol.* 236, 16–24. doi: 10.1016/j.taap.2008.12.023

Choi, J. S., Kim, R.-O., Yoon, S., and Kim, W.-K. (2016). Developmental toxicity of zinc oxide nanoparticles to zebrafish (*Danio rerio*): a transcriptomic analysis. *PLoS One* 11:e0160763. doi: 10.1371/journal.pone.0160763

Chueh, P. J., Liang, R. Y., Lee, Y. H., Zeng, Z. M., and Chuang, S. M. (2014). Differential cytotoxic effects of gold nanoparticles in different mammalian cell lines. *J. Hazard. Mater.* 264, 303–312. doi: 10.1016/j.jhazmat.2013.11.031

Compan, V., Baroja-Mazo, A., López-Castejón, G., Gomez, Ana, I., Martínez, Carlos, M., et al. (2012). Cell volume regulation modulates NLRP3 inflammasome activation. *Immunity* 37, 487–500. doi: 10.1016/j.immuni.2012.06.013

Costa, P. M., Neuparth, T. S., Caeiro, S., Lobo, J., Martins, M., Ferreira, A. M., et al. (2011). Assessment of the genotoxic potential of contaminated estuarine sediments in fish peripheral blood: laboratory versus *in situ* studies. *Environ. Res.* 111, 25–36. doi: 10.1016/j.envres.2010.09.011

Dedeh, A., Ciutat, A., Treguer-Delapierre, M., and Bourdineaud, J. P. (2015). Impact of gold nanoparticles on zebrafish exposed to a spiked sediment. *Nanotoxicology* 9, 71–80. doi: 10.3109/17435390.2014.889238

Doering, J. A., Wiseman, S., Beitel, S. C., Giesy, J. P., and Hecker, M. (2014). Identification and expression of aryl hydrocarbon receptors (AhR1 and AhR2) provide insight in an evolutionary context regarding sensitivity of white sturgeon (*Acipenser transmontanus*) to dioxin-like compounds. *Aquat. Toxicol.* 150, 27–35. doi: 10.1016/j.aquatox.2014.02.009

Edelbrock, M. A., Kaliyaperumal, S., and Williams, K. J. (2013). Structural, molecular and cellular functions of MSH2 and MSH6 during DNA mismatch repair, damage signaling and other noncanonical activities. *Mut. Res.* 743-744, 53–66. doi: 10.1016/j.mrfmmm.2012.12.008

Gamage, N., Barnett, A., Hempel, N., Duggleby, R. G., Windmill, K. F., Martin, J. L., et al. (2006). Human sulfotransferases and their role in chemical metabolism. *Toxicol. Sci.* 90, 5–22. doi: 10.1093/toxsci/kfj061

Garcia-Reyero, N., Thornton, C., Hawkins, A. D., Escalon, L., Kennedy, A. J., Steevens, J. A., et al. (2015). Assessing the exposure to nanosilver and silver nitrate on fathead minnow gill gene expression and mucus production. *Environ. Nanotechnol. Monit. Manag.* 4, 58–66. doi: 10.1016/j.enmm.2015.06.001

Geffroy, B., Ladhar, C., Cambier, S., Treguer-Delapierre, M., Brèthes, D., and Bourdineaud, J. P. (2012). Impact of dietary gold nanoparticles in zebrafish at very low contamination pressure: the role of size, concentration and exposure time. *Nanotoxicology* 6, 144–160. doi: 10.3109/17435390.2011.562328

Joubert, Y., Pan, J.-F., Buffet, P.-E., Pilet, P., Gilliland, D., Valsami-Jones, E., et al. (2013). Subcellular localization of gold nanoparticles in the estuarine bivalve *Scrobicularia plana* after exposure through the water. *Gold Bull.* 46, 47–56. doi: 10.1007/s13404-013-0080-2

Krähenbühl, O., and Tschopp, J. (1991). Perforin-induced pore formation. *Immunol. Today* 12, 399–402. doi: 10.1016/0167-5699(91)90139-K

Lamkanfi, M., and Dixit, V. M. (2011). Modulation of inflammasome pathways by bacterial and viral pathogens. *J. Immunol.* 187, 597–602. doi: 10.4049/jimmunol.1100229

Liu, X., Atwater, M., Wang, J., and Huo, Q. (2007). Extinction coefficient of gold nanoparticles with different sizes and different capping ligands. *Coll. Surfaces B Biointerfaces* 58, 3–7. doi: 10.1016/j.colsurfb.2006.08.005

Meland, S., Farmen, E., Heier, L. S., Rosseland, B. O., Salbu, B., Song, Y., et al. (2011). Hepatic gene expression profile in brown trout (*Salmo trutta*) exposed to traffic related contaminants. *Sci. Total Environ.* 409, 1430–1443. doi: 10.1016/j.scitotenv.2011.01.013

Odom, E. W., and Vasta, G. R. (2006). Characterization of a binary tandem domain F-type lectin from striped bass (*Morone saxatilis*). *J. Biol. Chem.* 281, 1698–1713. doi: 10.1074/jbc.M507652200

Ojea-Jimenez, I., Lopez, X., Arbiol, J., and Puntes, V. (2012). Citrate-coated gold nanoparticles as smart scavengers for mercury(II) removal from polluted waters. *ACS Nano* 6, 2253–2260. doi: 10.1021/nn204313a

O'Rourke, J. J., and Deans, A. J. (2016). "Chapter 12 - the FANCA to FANCZ of DNA interstrand crosslink repair: lessons from Fanconi anemia," in *DNA Repair in Cancer Therapy*, 2nd Edn, eds M. R. Kelley and M. L. Fishel (Boston: Academic Press), 353–381.

Pacheco, M., and Santos, M. (1996). Induction of micronuclei and nuclear abnormalities in the erythrocytes of *Anguilla anguilla* L. *exposed either to* cyclophosphamide or to bleached kraft pulp mill effluent. *Fresenius Environ. Bull.* 5, 746–751.

Paramelle, D., Sadovoy, A., Gorelik, S., Free, P., Hobley, J., and Fernig, D. G. (2014). A rapid method to estimate the concentration of citrate capped silver nanoparticles from UV-visible light spectra. *Analyst* 139, 4855–4861. doi: 10.1039/c4an00978a

Popp, L., and Segatori, L. (2015). Differential autophagic responses to nano-sized materials. *Curr. Opin. Biotechnol.* 36, 129–136. doi: 10.1016/j.copbio.2015.08.016

Portt, L., Norman, G., Clapp, C., Greenwood, M., and Greenwood, M. T. (2011). Anti-apoptosis and cell survival: a review. *Biochim. Biophys. Acta* 1813, 238–259. doi: 10.1016/j.bbamcr.2010.10.010

Singh, N. P., McCoy, M. T., Tice, R. R., and Schneider, E. L. (1988). A simple technique for quantitation of low levels of DNA damage in individual cells. *Exp. Cell Res.* 175, 184–191. doi: 10.1016/0014-4827(88)90265-0

Skov, S., Bregenholt, S., and Claesson, M. H. (1997). MHC class I ligation of human T cells activates the ZAP70 and p56lck tyrosine kinases, leads to an alternative phenotype of the TCR/CD3 zeta-chain, and induces apoptosis. *J. Immunol.* 158, 3189–3196.

Teles, M., Boltaña, S., Reyes-López, F., Santos, M. A., Mackenzie, S., and Tort, L. (2013). Effects of chronic cortisol administration on global expression of GR and the liver transcriptome in *Sparus aurata*. *Mar. Biotechnol.* 15, 104–114. doi: 10.1007/s10126-012-9467-y

Teles, M., Fierro-Castro, C., Na-Phatthalung, P., Tvarijonaviciute, A., Trindade, T., Soares, A. M., et al. (2016). Assessment of gold nanoparticle effects in a marine teleost (*Sparus aurata*) using molecular and biochemical biomarkers. *Aquat. Toxicol.* 177, 125–135. doi: 10.1016/j.aquatox.2016.05.015

Teles, M., Soares, A. M. V. M., Tort, L., Guimarães, L., and Oliveira, M. (2017). Linking cortisol response with gene expression in fish exposed to gold nanoparticles. *Sci. Total Environ.* 58, 1004–1011. doi: 10.1016/j.scitotenv.2017.01.153

Truong, L., Tilton, S. C., Zaikova, T., Richman, E., Waters, K. M., Hutchison, J. E., et al. (2013). Surface functionalities of gold nanoparticles impact embryonic gene expression responses. *Nanotoxicology* 7, 192–201. doi: 10.3109/17435390.2011.648225

Xin, Q., Rotchell, J. M., Cheng, J., Yi, J., and Zhang, Q. (2015). Silver nanoparticles affect the neural development of zebrafish embryos. *J. Appl. Toxicol.* 35, 1481–1492. doi: 10.1002/jat.3164

Zhang, X.-D., Wu, D., Shen, X., Liu, P.-X., Yang, N., Zhao, B., et al. (2011). Size-dependent in vivo toxicity of PEG-coated gold nanoparticles. *Int. J. Nanomed.* 6, 2071–2081. doi: 10.2147/IJN.S21657

Conflict of Interest Statement: The authors declare that the research was conducted in the absence of any commercial or financial relationships that could be construed as a potential conflict of interest.